



BRILL

Multidiscipline Modeling in Mat. and Str. 4(2008)XX-XX

MMMS

www.brill.nl/mmms

APPLICATION OF TOPOLOGY, SIZE AND SHAPE OPTIMIZATION METHODS IN POLYMER METAL HYBRID STRUCTURAL LIGHTWEIGHT ENGINEERING

¹M. Grujicic, G. Arakere, P. Pisu, B. Ayalew, ²Norbert Seyr, ³Marc Erdmann and Jochen Holzleitner

¹Department of Mechanical Engineering Clemson University, Clemson SC 29634

²BMW Group, Research and Technology, Knorrstraße 147 80788 München, Germany

³BMW AG, Forschungs- und Innovationszentrum, Knorrstraße 147 80788 München, Germany

¹241 Engineering Innovation Building, Clemson, SC 29634-0921;

Phone: (864) 656-5639, Fax: (864) 656-4435, E-mail: mica.grujicic@ces.clemson.edu

Received 13 September 2006; accepted 18 October 2006

Abstract

Application of the engineering design optimization methods and tools to the design of automotive body-in-white (BIW) structural components made of polymer metal hybrid (PMH) materials is considered. Specifically, the use of topology optimization in identifying the optimal initial designs and the use of size and shape optimization techniques in defining the final designs is discussed. The optimization analyses employed were required to account for the fact that the BIW structural PMH component in question may be subjected to different in-service loads be designed for stiffness, strength or buckling resistance and that it must be manufacturable using conventional injection over-molding. The paper demonstrates the use of various engineering tools, i.e. a CAD program to create the solid model of the PMH component, a meshing program to ensure mesh matching across the polymer/metal interfaces, a linear-static analysis based topology optimization tool to generate an initial design, a non-linear statics-based size and shape optimization program to obtain the final design and a mold-filling simulation tool to validate manufacturability of the PMH component.

Keywords

Topology, Size and Shape Optimization, Polymer Metal Hybrid Structural, Lightweight Engineering

1. Introduction

Lightweight engineering for automobiles is progressively gaining in importance in view of rising environmental demands and ever-tougher emissions standards. Current efforts in the automotive lightweight engineering involve at least the following five distinct approaches [1]: (a) Requirement lightweight engineering which includes efforts to

reduce the vehicle weight through reductions in component/subsystem requirements (e.g. a reduced required size of the fuel tank); (b) Conceptual lightweight engineering which includes the development and implementation of new concepts and strategies with potential weight savings such as the use of a self-supporting cockpit, a straight engine carrier, etc.; (c) Design lightweight engineering which focuses on design optimization of the existing components and sub-systems such as the use of ribs and complex cross-sections for enhanced component stiffness at a reduced weight; (d) Manufacturing lightweight engineering which utilizes novel manufacturing approaches to reduce the component weight while retaining its performance (e.g. a combined application of spot welding and adhesive bonding to maintain the stiffness of the joined sheet-metal components with reduced wall thickness); and (e) Material lightweight engineering which is based on the use of materials with a high specific stiffness and/or strength such as aluminum alloys and polymer-matrix composites or a synergistic use of metallic and polymeric materials in a hybrid architecture (referred to as polymer metal hybrids, PMHs, in the remainder of this manuscript). In the present work, the problem of integration of the engineering optimization methods and tools into the aforementioned lightweight engineering efforts, specifically into PMH technology for body-in-white (BIW) load-bearing automotive components processed by techniques such as injection over-molding [2] or metal over-molding [3]. Such components are typically designed for stiffness and buckling resistance and their performance is greatly affected by the design of the plastic ribbing structure injection molded into a sheet-metal stamping.

In conventional automotive manufacturing practice, metals and plastics are fierce competitors. The PMH technologies, in contrast, aspire to take full advantage of the two classes of materials by combining them in a single component/sub-assembly. The first example of a successful implementation of this technological innovation in practice was reported at the end of 1996, when the front end of the Audi A6 (made by Ecia, Audincourt/France) was produced as a hybrid structure, combining sheet steel with elastomer-modified poly-amide PA6 - GF30 (Durethan BKV 130 from Bayer). A key feature of hybrid structures is that the materials employed complement each other so that the resulting hybrid material can offer an enhanced overall structural performance. Currently, PMHs are replacing all-metal structures in automotive front-end modules at an accelerated rate and are being used in instrument-panel and bumper cross-beams, door modules, and tailgates applications. Moreover, new PMH technologies are being introduced.

The main PMH technologies currently being employed in the automotive industry can be grouped into three major categories: (a) Injection over-molding technologies [2]; (b) Metal-over-molding technologies combined with secondary joining operations [3]; and (c) Adhesively-bonded PMHs [4]. A detailed description for each of these groups of PMH manufacturing technologies can be found in our recent work [5]. Hence, only a brief overview of each is given below.

In the injection over-molding process, metal inserts with flared through-holes are stamped, placed in an injection mold and over-molded with short-glass reinforced thermoplastics to create a cross-ribbed supporting structure. The metal and plastics are joined by the rivets which are formed by the polymer melt penetrating through-holes in the metal stamping(s). Such rivets than provide mechanical interlocks between the plastics and the metal. In the metal over-molding PMH technology, a steel stamping is placed in an injection mold, where its underside is coated with a thin layer of reinforced

thermoplastics. In a secondary operation, the plastics-coated surface of the metal insert is ultrasonically welded to an injection molded glass-reinforced thermoplastic sub-component. In this process, a closed-section structure with continuous bond lines is produced which offers a high load-bearing capability. In the adhesively-bonded PMH technology, glass-fiber reinforced poly-propylene is joined to a metal stamping using Dow's proprietary low-energy surface adhesive (LESA) [4]. The acrylic-epoxy adhesive does not require pre-treating of the low surface-energy poly-propylene and is applied by high-speed robots. Adhesive bonding creates continuous bond lines, minimizes stress concentrations and acts as a buffer which absorbs contact stresses between the metal and polymer sub-components. Adhesively-bonded PMHs enable the creation of closed-section structures which offer high load-bearing capabilities and the possibility for enhanced functionality of hybrid parts (e.g. direct mounting of air bags in instrument-panel beams or incorporation of air or water circulation inside door modules). In addition to these PMH technologies, the potential for a so called direct-adhesion PMH technology in which the joining between the metal and injection-over-molded thermoplastic sub-components is attained through direct polymer-to-metal adhesion without the use of inter-locking rivets/over-molded edges or structural adhesives was discussed in our recent work [5].

Due to ever-more restrictive lightweight targets and the demands for shortened product development time scale in the automotive industry, a continues need has arisen for an integration of advanced computer aided optimization methods into the overall component/sub-assembly design process. This is particularly true in the case of structural load-bearing PMH BIW automotive components (e.g. rear longitudinal beams, cross-roof beams, etc.). In the present work, we explore the use of Altair's OptiStruct topology, sizing and shape structural optimization program [6]. In most cases, the design of the load-bearing PMH components is driven by stiffness and buckling requirements but also by strength requirements (e.g. to obtain the required performance in side-impact collisions). These multiple requirements placed on a single component will be addressed in the present work. Since the BIW load-bearing PMH components are often designed for buckling resistance and must be manufacturable by injection-over-molding, the use of non-linear structural analysis and size and shape optimization program Abaqus [7] and a mold-filling simulation program Moldflow Plastics Insight [8] is also explored.

Finite-element analysis based topology, size and shape optimization methods and tools are typically used as part of a two-phase product-design process: (a) Topology optimization is performed first to obtain a rough idea about an optimal configuration for the product at hand, i.e. to obtain an initial design with optimal load paths; and (b) the configuration suggested in (a) is next interpreted to form an engineering design which is then optimized using detailed size and shape optimization methods and tools with real design requirements. Numerous examples from the automotive industry have demonstrated the ability of such an approach to quickly generate optimized all-metal components for stiffness, stress and vibration based designs [8]. Such approach is not as frequently used in the design of PMH components since additional manufacturability constraints have to be included in the design optimization scheme.

The success of the above optimization scheme relies on a topology optimization to suggest a good initial design. Numerous examples have shown that major weight savings are achieved when selecting the initial design and only minor additional weight

savings are attained when subsequent detailed size and shape optimization of the initial design is carried out. The automotive industry is fully aware of this and, over the years, considerable in-house body of knowledge has been acquired pertaining to the optimal design of different BIW load-bearing components. Nevertheless, topology optimization methods may still have a place as new sizes/types of vehicles are designed and as new materials and manufacturing processes (e.g. the PMH technologies) continue to appear. In the present work, an attempt is made to promote the use of engineering optimization in the design of BIW load-bearing PMH components.

The objective of the present work is to extend the aforementioned two-step optimization approach to BIW load bearing PMH components. A typical all-metal BIW load bearing component, Figure 1(a), consists of two flanged U-shape stampings joined along their matching flanges by spot-welding (often complemented by adhesive bonding). When such an all-metal component is replaced with a PMH component, Figure 1(b), one of its stampings is removed and the exterior of the remaining stamping reinforced using an injection-molded thermoplastic rib-like structure. Hence, the objective of the present work is to address the optimal architecture of the ribbing structure with respect to different loading requirements (axial compression, bending, twisting) and different design requirements (e.g. stiffness, strength, buckling resistance). The examples considered show how topology optimization may be used to suggest good initial designs, but also demonstrates how a topology optimization followed by a detailed size and shape optimization may be used to provide efficient designs satisfying performance and manufacturing constraints.

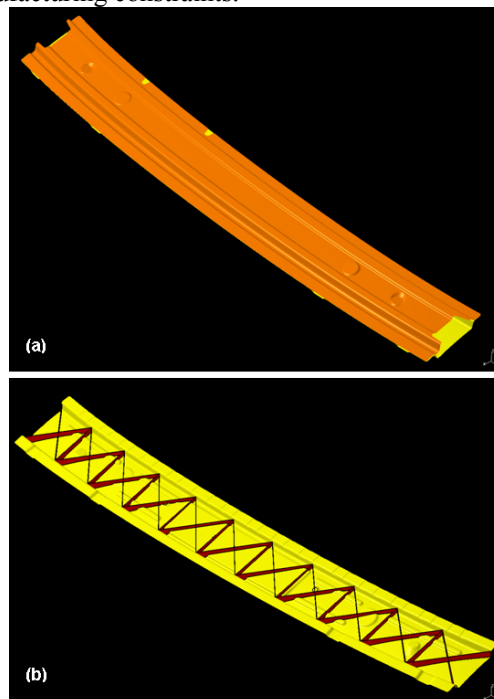


Fig.1 (a) A twin-shell all-metal rear cross-roof member and (b) its polymer metal hybrid counterpart consisting a single metal-shell stamping and injection-molded plastic ribbing.

The organization of the paper is as follows: An overview of the basics of topology, size and shape optimization methods is presented in Section II. 1. A brief description of the main computational tools used in the present work is given in Section II.2. The results obtained in the present work are presented and discussed in Section III. The main conclusions resulting from the present work are summarized in Section IV.

2. Computation Procedure

2.1 The Basics of Structural Topology, Size and Shape Optimization

Structural optimization is a class of engineering optimization problems in which the evaluation of an objective function(s) or constraints requires the use of structural analyses (typically a finite element analysis, FEA). In compact form, the optimization problem can be symbolically defined as [9]:

Minimize the objective function $f(x)$

Subject to the non-equality constraints $g(x) < 0$ and to the equality constraints $h(x) = 0$

Where the design variables x belong to the domain D where, in general, $g(x)$ and $h(x)$ are vector functions. The design variables x form a vector of parameters describing the geometry of a product. For example, x , $f(x)$, $g(x)$ and $h(x)$ can be product dimensions, product weight, a stress condition defining the onset of plastic yielding, and constraints on product dimensions, respectively. Depending on the nature of design variables, its domain D can be continuous (e.g. a continuous range of the length of a bar), discrete (e.g. the standard gage thicknesses of a plate or the existences of structural member in a product), or the mixture of the two. Furthermore, a structural optimization may have multiple objectives, in which case the objective function becomes a vector function.

Structural optimizations are typically classified according to the following three viewpoints: (a) The type of analysis used (e.g. linear static stress/displacement analysis, natural frequencies and normal modes analysis, buckling analysis, etc.); (b) Area of application (e.g. mechanical engineering, civil engineering, automotive engineering, etc.) and (c) Objectives of the optimization effort (e.g. geometry parameterization and optimization, development of optimization algorithms, etc.).

In the present work, the application of linear and non-linear static structural analyses for the optimization of BIW load-bearing PMH components via the application of the existing topology, size and shape optimization methods is considered. These methods are briefly overviewed in the remainder of this section.

Topology Optimization

Topology optimization methods allow the changes in the way substructures are connected within a fixed design domain and can be classified as (a) discrete element (also known as the ground structure) approach; and (b) continuum approaches. In the discrete element approach, the design domain is represented as a finite set of possible locations of discrete structural members such as truss, frame, and panels. By varying the width/thickness of each member in the design domain between zero (in this case the

element becomes nonexistent) and a certain maximum value, structures with different sizes and topologies can be represented. In the continuum approach, the design domain is represented as the continuum mixture of a material and “void” and the optimal design is defined with respect to the distributions of the material density within the design space. Since the discrete element approach utilizes a collection of primitive structural members, it allows easy interpretation of the conceptual design. However, potentially optimal topologies may not be attainable by the number and types of possible member locations defined in the design domain. The continuum approach, on the other hand, does not have this limitation, while it may be computationally more expensive. Over the last decades, major advances have been reported in the area of the discrete element structural optimization [10-16]. A continuum approach to topology optimization was first proposed by Bendsøe and Kikuchi [17] who developed the so called *Homogenization Design Method* (HDM). A comprehensive overview of the HDM can be found in Ref. [18]. Typical applications of this method can be found in Refs. [19-32].

Size Optimization

Within size optimization approach, the dimensions that describe product geometry are used as design variables, x . The application of size optimization is, consequently, mostly used at the detailed design stage where only the fine tuning of product geometry is necessary. Size optimization is typically done in conjunction with feature-based variation geometry [33] which is available in many modern CAD programs. With present-day availability of fast personal computers, size optimization is relatively a straightforward task and it typically requires no re-meshing of the finite element models during optimization iterations. A difficulty may arise, however, when extremely large finite element models or highly nonlinear phenomena need to be analyzed, in which case surrogate (simplified) models are typically employed.

Shape Optimization

Shape optimization allows the changes in the boundary of product geometry. The boundaries are typically represented as smooth parametric curves/surfaces, since irregular boundaries typically deteriorate the accuracy of finite element analysis or may even cause the numerical instability of optimization algorithms. Since product geometry can change dramatically during the optimization process, the automatic re-meshing of finite element models is usually required. Structural shape optimization methods are generally classified as: (a) direct geometry manipulation and (b) indirect geometry manipulation approaches. In the direct geometry manipulation approaches, design variable x is a vector of parameters representing the geometry of product boundary, e.g., the control points of the boundary surfaces. In the indirect geometry manipulation approaches, design variable x is a vector of parameters that indirectly defines the boundary of the product geometry. A comprehensive review of shape optimization based on the direct and the indirect geometry manipulation approaches can be found in Ref. [34]. The direct geometry manipulation approaches had been implemented in a number of commercial software such as OptiStruct [6].

The most widely used indirect geometry manipulation approach is the so-called *Natural Design Variable* method originally developed by Belegundu and Rajan [35],

which uses fictitious loads applied on the boundaries of the product geometry as design variables.

In each iteration, a new boundary is obtained by adding the displacements induced by these fictitious loads to the original boundary. Since the displacements are calculated by finite element methods based on force equilibrium, the resulting new boundary tends to be smoother and less likely to have heavily distorted meshes, than the ones obtained by the direct geometry manipulation approaches. On the other hand, imposing geometric constraints on product boundary is more complicated than in direct geometry manipulation, since the constraints must be expressed as the corresponding fictitious loads. Variants of the *Natural Design Variable* method have been implemented in a number of commercial programs, such as Nastran [36] and Abaqus [7]. It should be also mentioned that there are several hybrid shape optimization methods which try to combine the advantages of the direct and indirect geometry manipulation approaches [37, 38].

In conclusion, it should be recognized that, in addition to maximization of the stiffness and strength based structural efficiency, size and shape optimization methods have been applied to numerous areas of concern in mechanical product developments, including vibrations [39-41], crashworthiness [42-51], thermo-mechanical design [52], structural acoustics [53], structure-electro-magnetics [54], fluid/structure interactions [55], compliant mechanisms [56-58], micro-electro-mechanical systems [59-63], and reliability optimization [64-67].

2.2 Computer Engineering Tools Used in the Present Work

As stated earlier, the main objective of the present work is to demonstrate and promote the use of engineering optimization methods and tools to generate optimal and manufacturable BIW load-bearing PMH components. However the full integration of this procedure into the component-design process, entails the use of additional methods and tools. Such methods and tools are briefly discussed below.

Computer Aided Design (CAD)

The starting point in the procedure used in the present work is the use of a CAD program to generate the initial design of the metal stamping and the design space (initially) filled with the thermoplastic material. To enable easy redesign of the metal stamping and the polymer-based design space, a parametric-type of CAD program is generally preferred. In the present work Catia version 5 from Dassault Systems [68] was used. It should be noted that Catia is not only a parametric solid/surface based CAD package but also an integrated suite of CAD, Computer Aided Engineering (CAE) and (primarily metal-based) Computer Aided Manufacturing (CAM) application tools.

Meshing Program

Since the design optimization procedure discussed in Section II.1 (generally) employ various finite element analysis, meshing of the CAD represented PMH component is required. While CAD programs like Catia provide part-meshing capabilities, such capabilities are relatively limited and do not readily enable mesh-matching across the part/part (polymer/metal, in the present case) interfaces. Such mesh-matching is important in the PMH component to ensure a “seamless” transfer of loads across

polymer/metal interfaces. To overcome this limitation of the CAD program, the high-performance pre-and post-processing CAE software program, HyperMesh from Altair [6] is used in the present work.

Linear Elastic Static Analysis Based Optimization

When a BIW load-bearing PMH component is designed for stiffness (i.e. maximum allowable deflection is limited) or for strength (i.e. the maximum Von Mises stress is not allowed to exceed a specific fraction of the material yield strength) a linear-elastic static analysis-based topology, size and shape optimization can be used. Such optimization was carried out in the present work using OptiStruct program from Altair [6]. It should be noted that OptiStruct also has the capabilities to carry out a linearized buckling analysis. However, the linearized buckling analysis is an approximate analysis since it does not take into account the effect of geometrical and material non-linearities, which often can significantly affect the magnitude of buckling loads.

Non-Linear Elastic Buckling Optimization Analysis

When a BIW load-bearing component is designed for buckling resistance (i.e. the component should be able to support a maximum loading before the onset of buckling), the underlying structural analysis is non-linear in character and OptiStruct cannot be used. To overcome this problem, Abaqus non-linear finite element analysis and size and shape optimization program [7] is used in the present work. Since Abaqus cannot be used to carry out topology optimization of the PMH component, optimization for buckling is first carried out using OptiStruct linearized buckling analysis. Since, it is generally found that a component optimized using the linearized buckling analysis possesses a high (not a maximum) resistance to buckling, the PMH component topology optimized for buckling using OptiStruct is next (size and shape) optimized for buckling resistance using Abaqus.

Manufacturability Validation Tool

As stated earlier, the final design of the BIW load-bearing PMH component should be manufacturable using standard injection-over-molding. To validate such manufacturability of the final design, MoldFlow Plastics Insight (version 6.1), mold-filling simulation program from MoldFlow Corporation [8] is used in the present work. This program gives insight into the following aspects of the injection molding process: filling time, incomplete filling, weld lines, air traps, local fiber orientation, etc. All these factors are used in judging manufacturability and quality of an injection over-molded PMH component.

3. Results and Discussion

To demonstrate the use of structural optimization in the design of BIW load-bearing PMH components, a proto-typical twin-shell flanged U-shape 0.7mm-thick stamped-metal component made of a dual-phase steel (Young's modulus = 210 GPa, yield strength = 350 MPa) is analyzed in the remainder of this manuscript. The lower and the upper stampings are joined using 5mm-diameter/3mm-apart spot welds. The relevant dimension of the all-metal BIW component are displayed in Figure 2(a). It should be

noted that, in order to reduce the computational cost, the length of the BIW component is substantially reduced relative to a typical real BIW-frame component.

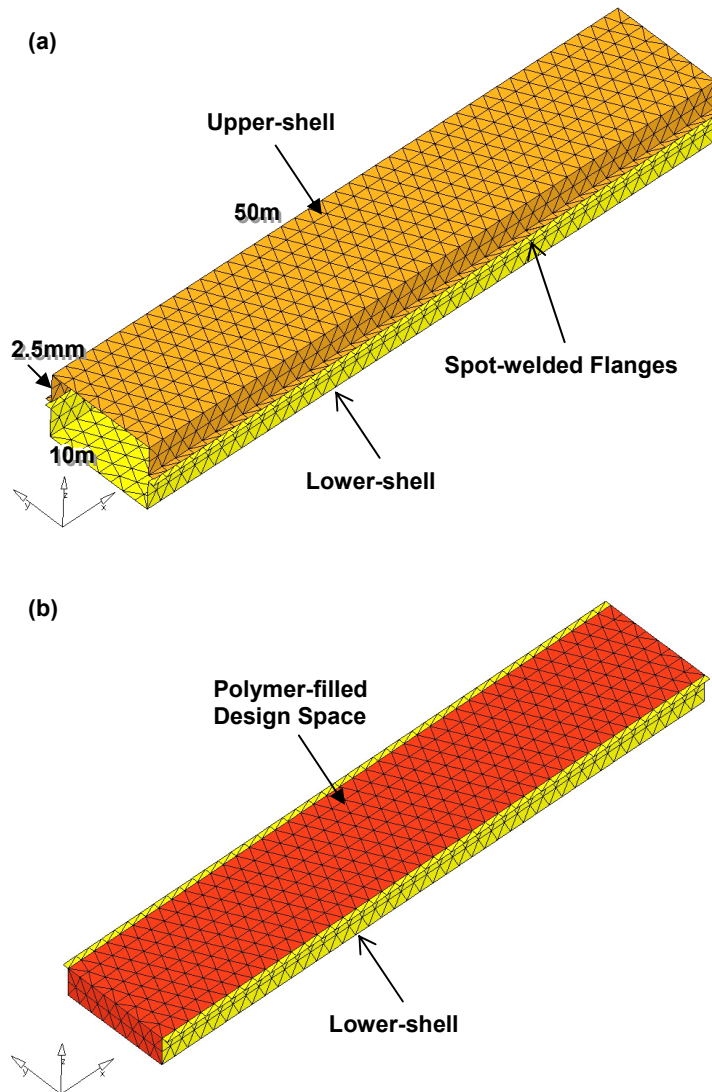


Fig 2 (a) A prototypical twin-shell all-metal BIW load-bearing component; and (b) the initial configuration of the corresponding PMH component

The upper twin-stamping (used in the aforementioned all-metal construction) is next removed and is replaced with an injection-molded thermoplastic-polymeric sub-structure. Since the resulting PMH component is an integral part of the BIW frame and, hence, must be able to withstand thermal exposures during BIW construction by joining (primarily by spot and fusion welding) and the BIW pre-treatment and painting

operations (in particular, the 190-200°C, 20-30 minute E-coat baking treatment), a thermally-stabilized poly-amide (nylon) 6 containing ca. 30 wt. % of glass fibers is used as the thermoplastic-polymeric material. The relevant properties of this material are: Young's modulus = 9.0 GPa, yield strength = 0.5 MPa, density = 1.35 g/mm³, injection-molding temperature = 290°C, melt viscosity = 200Pa·s at the injection-molding temperature. The other properties of this material can be found in our previous work [5].

Structural optimization discussed in the present work may be viewed as a problem of finding the design with optimal load paths for well-defined loads from their application positions to well-defined supports. Individual BIW load-bearing components are normally integrated into a larger structure (the BIW) and, consequently, the loads experienced by the component are not fixed. In other words, the component design and the method of its joining to the adjacent components will affect how loads diffuse into the component. This implies that structural optimization of a BIW component should be carried out in the context of the overall BIW design. This approach is being used in our ongoing research [69]. In the present work, for the purpose of demonstrating the use of various optimization and process-modeling methods and tools in the development of BIW load-bearing PMH components, a fixed set of loads is considered during the optimization process.

To establish the basis for the definition of the optimization constraints, the all-metal component is first loaded (in axial compression, two bending modes and twisted along its longitudinal axis) and the resulting maximum deflections, maximum von Mises stresses and buckling loads recorded for each loading case. The recorded deflections are then defined as the optimization constraints in a stiffness-based design of the corresponding PMH component. In other words, the stiffness-based design-optimization problem is defined as minimization of the PMH-component weight (via the reduction of the volume of the thermo-plastic material and via the optimization of topology, size and shape of the component) subjected to the constraints that, when the component is subjected to the same loads as its all-metal counterpart, its maximum deflections do not exceed the corresponding ones in the all-metal counterpart. Similarly, the maximum von Mises stresses and buckling loads are respectively used in strength and buckling-based design-optimization analyses of the same PMH component.

As discussed earlier, a typical BIW load-bearing PMH component consists of a flanged U-shape metal stamping which is (using various means) coupled with an injection-molded (typically glass-fiber reinforced) thermoplastic-polymer sub-component. In the present work, the direct adhesion injection-over-molding process for the PMH-component manufacture is considered. Within such a process, the U-shaped metal-stamping is placed into the injection-molding mold, the mold is closed and the fiber-reinforced thermoplastic melt injection molded against the metal stamping to produce a stiffening and buckling-delaying rib-like structure. The needed level of polymer-to-metal adhesion is achieved by a combination of the stamping surface treatment and chemical modifications of the thermoplastic material.

3.1 Conceptual Design of BIW Load-bearing PMH Components

To determine the initial design of the PMH component using topology optimization, the metal stamping is first filled completely with polymer and the resulting hybrid-structure meshed, Figure 2(b). Next, the plastics region is declared as the design space, and the topology optimization carried out using OptiStruct. As discussed earlier,

different loading modes (i.e. axial compression, two bending modes and axial torsion) and different optimization constraints (i.e. stiffness, strength and buckling resistance) are considered. It should be also noted that throughout all the structural analysis carried out in the present work, perfect adhesion is assumed to exist between the metal and the polymer. In our previous work [5], the effect of the polymer-to-metal adhesion strength on the functional performance of the PMH components was addressed. The results obtained showed that in order to attain the needed load transfer between the metal and the plastics, minimum adhesion strength of ~ 10 MPa is required. Furthermore, it was found that, when the adhesion strength is ≥ 10 MPa, the structural analysis results are practically identical to those corresponding to the perfect polymer-to-metal adhesion.

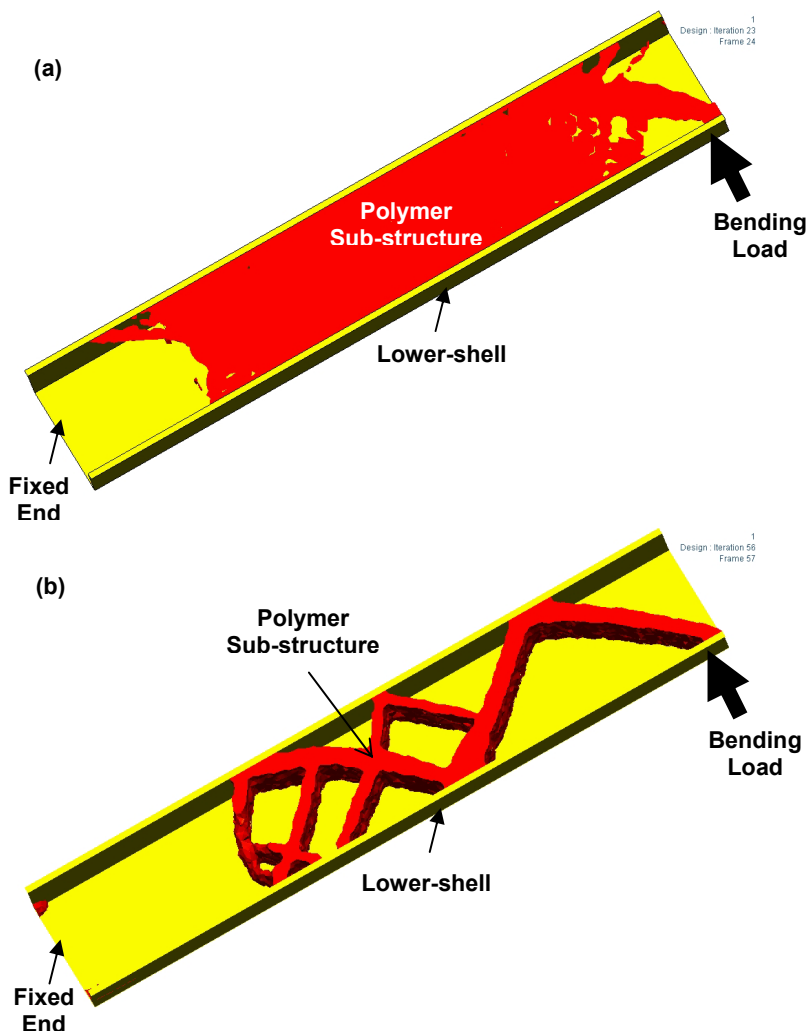


Fig.3 A Figure 3 Optimal stiffness-based topology for the prototypical PMH component with respect to bending: (a) without; and (b) with injection-over molding manufacturing constraints.

The results of the topology optimization analysis for the case of stiffness-based design under bending load are displayed (using a homogenized polymer/void material density plot) in Figure 3(a). In other words, the topology displayed in Figure 3(a) corresponds to the region in the design space whose density is at least 90% of the density of the plastic material. The results displayed in Figure 3(a) indicate that the optimal structure of the injection-molded polymer is a plate like structure located at the open (longitudinal) side of the U-shape stamping. In other words, the PMH component acquires a close-box shape, the shape which is known as one of the structurally most efficient cross-sectional shapes.

The configuration displayed in Figure 3(a) cannot be easily manufactured using injection over-molding approach. This is caused by the fact that in a standard two-part mold injection over-molding process, the metal stamping is placed and secured in one half of the mold, the mold is closed by translating the other half of the mold in a direction normal to the length of the part. Thermoplastic melt is subsequently injected into the mold and against the surfaces of the metal stamping. In the PMH-part topology displayed in Figure 3(a), (at least) a third part of the mold has to be introduced with a motion along the length of the part. This would make the injection molding process cumbersome and the tooling very expensive. To overcome this problem, injection molding-manufacturing constraints are included into the PMH-part topology optimization. Specifically, it is stated that the traveling of the moving-half of the mold is in a direction normal to the bottom face of the flanged U-shape stamping. With this manufacturing-based constraint added, the topology optimization is run again using OptiStruct and the results of this analysis are displayed in Figure 3(b). In this case, as seen in Figure 3(b), one can clearly discern the formation of ribs in the design space.

To show that the optimal topology of the PMH component is sensitive to the nature of (mechanical) constraints used (i.e., stiffness-based vs. strength-based design), the aforementioned procedure is repeated but the mechanical constraint is defined by the condition that the von-Mises stress should not exceed 50% of the yield strength of the thermo-plastic material. The results of this optimization without and with the application of the injection over-molding constraints are displayed in Figures 4(a)-(b). As in the case of the aforementioned stiffness-based optimization, a close-box shape is preferred, when the manufacturability constraints are not imposed, and a rib-like substructure, when the manufacturability constraints are applied. However, there are clear differences in the corresponding results presented in Figures 3(a)-(b) and 4(a)-(b). Among these differences, the two most apparent ones are: (a) In the case of strength-based designs, figures 4(a)-(b), the thermoplastic substructure extends all the way to the fixed end of the PMH component. No such extension is seen in the case of stiffness-based design, Figure 3(a)-(b); and (b) In the case of stiffness-based design, Figure 3(a)-(b), the thermoplastic substructure is primarily concentrated in the (lengthwise) middle section of the PMH component. These two observations are consistent with the fact that the largest stresses are encountered at the fixed end of the PMH component and that the magnitude of the free-end deflection is primarily controlled by the stiffness of its (lengthwise) middle section.

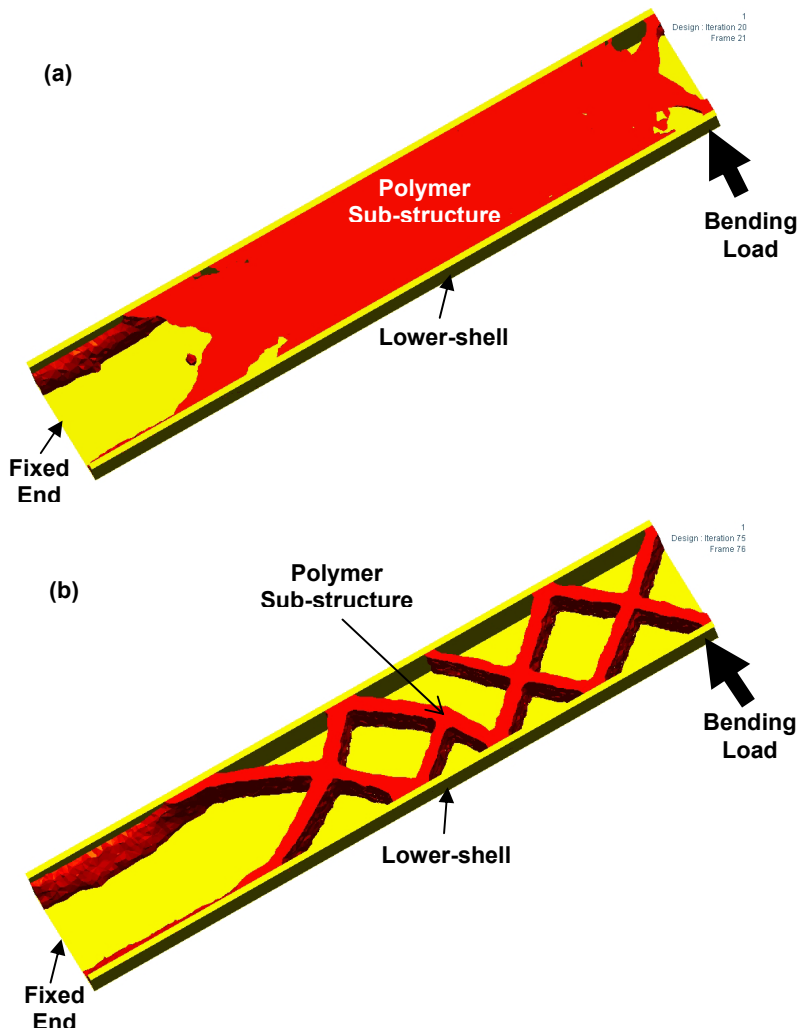


Fig.4 Optimal strength- based topology for the prototypical PMH component with respect to bending: (a) without; and (b) with injection-over molding manufacturing constraints.

The finite element analyses used in the stiffness- and strength-based optimizations presented above are of a linear static nature and can be carried out using OptiStruct. However, as pointed out earlier, many BIW load-bearing automotive components are designed for buckling resistance and buckling analysis is non-linear in nature. To overcome this limitation, a procedure is proposed and applied to the PMH component in Section III.3.

3.2 Final Design of BIW Load-bearing PMH Components

Once the conceptual design of the PMH component is completed through the use of topology optimization, such design can be imported into a parametric CAD program (Catia, in the present work) and converted into a geometrical model suitable for further size and shape optimizations. Such optimizations were done in the present work using OptiStruct, except for the cases when the design was buckling-resistance based. The procedure used in the case of buckling-resistance based design is presented in next section. The optimal stiffness-based and strength-based final designs corresponding to the optimal topologies displayed in Figures 3(b) and 4(b) are shown in Figures 5(a)-(b), respectively. It should be noted that local wall-thicknesses of the injected-molded polymer were used as the design variables in the size optimization analyses, while the vertical coordinates of the nodes defining the (top) rim of the ribs were used as the design variables in the (linear-base function) shape optimization analysis. It should be noted that the optimized rib-rims acquired a planar shape since the vertical location of the rim nodes was not allowed to exceed that of the metal-shell flange nodes.

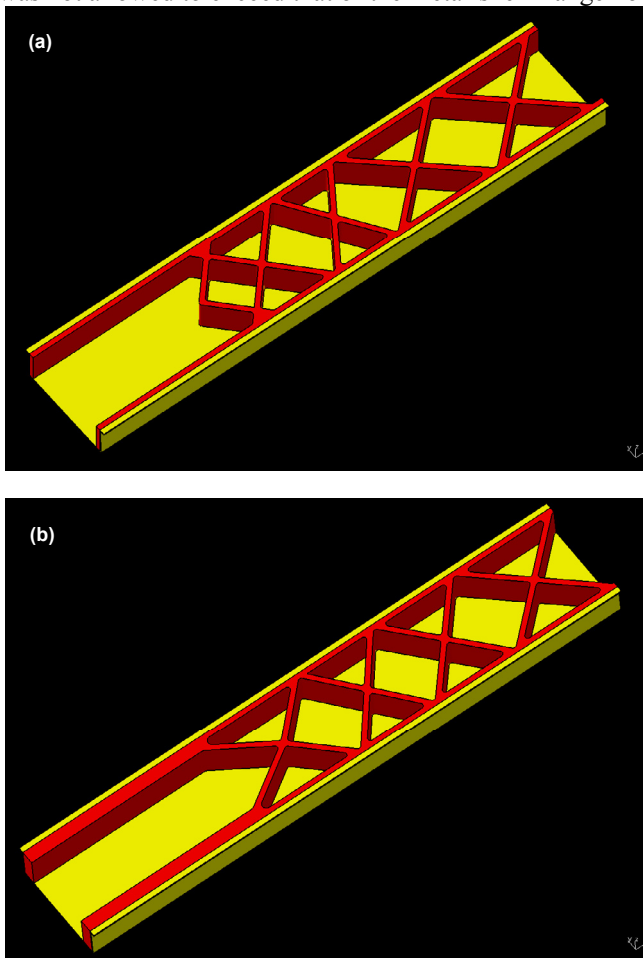


Fig.5 Final: (a) stiffness-based and (b) strength-based final optimal design for the prototypical PMH component subjected to bending.

The procedure carried out above showed that the conceptual design typically yields a weight reduction of ~15-20% relative to the all-metal counterpart while the final (size and shape) design modifications result in only ~2-4% additional weight reductions.

3.3 Buckling Resistance-based Design of BIW Load-bearing PMH

Components

Due to their thin-wall structure, a number of BIW load-bearing components are more likely to fail by buckling (elastic instability) than by plastic deformation. Consequently such components are designed for buckling resistance rather than for strength. As discussed earlier buckling-resistance based optimization of the BIW load-bearing components is done in two steps; (a) topology optimization is done using a linearized buckling analysis within OptiStruct [7]; and (b) the final size and shape optimization is carried out using a non-linear optimization procedure within Abaqus [38]. The two buckling analysis are first briefly reviewed below and then applied to the proto-typical BIW load-bearing PMH component considered in this manuscript.

The linearized (eigenvalue) buckling analysis is based on the use of the initial stiffness matrix of the system. The analysis is carried out in three distinct steps: (a) First a static analysis is carried out under an arbitrary ordinate loading to determine the initial stiffness matrix $[K_e]$ corresponding to the ‘base state’ of the system; (b) The loading is next applied and the corresponding loading induced incremental stiffness $[K_g]$ determined; and (c) At last, the conditions under which the overall stiffness matrix of the system becomes singular is defined i.e. the following eigenvalue problem is set up and solved:

$$\{[K_e] + \lambda_i [K_g]\} \{u_i\} = \{0\} \quad (1)$$

where λ_i ($i=1,2,\dots$) are the eigenvalues, $\{u_i\}$ the corresponding buckling mode shapes. The buckling loads are then simply found by multiplying the reference loads with the corresponding eigenvalues.

As mentioned earlier, the linearized buckling eigenvalue analysis presented above is only approximate since it does not take into account the effect of the geometrical and (or material nonlinearity). To overcome this problem, a general non-linear buckling analysis based on the load-deflection Riks method is carried out. Within the Riks method, loading is proportional, i.e. at any instant, the ratio of the current magnitude of any loading component and its reference value is the same. Furthermore, in addition to solving for the displacements during the finite element analysis, within the Riks method the load magnitude is also defined as an unknown and is solved for. The progress of the analysis is monitored using the arc length of the load vs. displacement curve. In general, Riks method provides the solution to the problem regardless whether the response of the structure is stable (i.e. load increases with an increase in the corresponding displacement) or unstable (i.e. when the stiffness becomes negative and the structure must release strain energy in order to remain in equilibrium). As mentioned above, Riks analysis yields the current value of the load proportionality factor. Hence the buckling load is simply a product of the maximum load proportionality factor and the corresponding reference load.

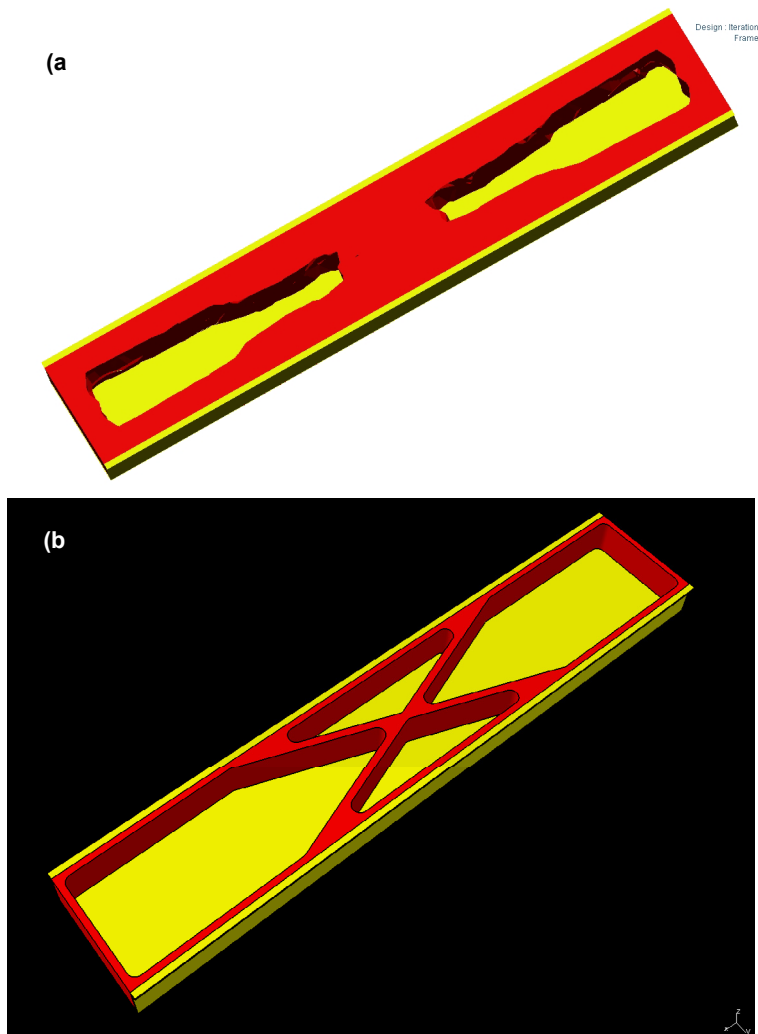


Fig.6 (a) Linearized buckling Eigen value-based conceptual design and (b) non-linear buckling-based final design for the prototypical PMH component within injection over-molding.

As stated earlier, the topology, size and shape optimizations for the buckling resistance based design were first carried out in OptiStruct using the linearized eigenvalue buckling analysis. To further optimize the design for potential non-linear geometrical and material effects, Abaqus Standard finite element program was used. It was found that, in general, the linearized buckling analysis yield the design which is quite close to that obtained using more-general (and computationally quite more expensive) non-linear buckling analysis. An example of the optimal design obtained using OptiStruct and Abaqus is displayed in Figures 6(a)-(b), respectively. It should be noted that the buckling analysis was carried out under axial compression loading condition.

3.4 Manufacturability of BIW Load-bearing PMH Components

Once the BIW load-bearing PMH component is designed using the topology, size and shape optimization methods and tools presented in the previous sections one must verify that the component can be manufactured using the standard injection over-molding technology and that the component is free of flaws (e.g. weld lines, entrapped air, incompletely-filled sections, excessive in-mold residual stresses which can cause distortions/warping of the PMH component after ejection from the mold, etc.). Such manufacturability (by injection over-molding) analysis is carried out in the present work using Moldflow Plastic Insight computer program [8]. Since a detailed discussion pertaining to the use of this program was presented in our recent work [5], only a brief overview is given here.

Within Moldflow, mass, momentum and energy conservation equations are solved numerically to model the processes associated with polymeric-melt mold filling, mold packing, melt solidification, polymer reinforcing-fiber orientation distribution, in-mold residual stress development, etc. To carry out the manufacturability analysis, the final design of the PMH component presented in the previous sections are directly imported in Moldflow, runner system and gates constructed, a cooling system provided (if required) and a mold filling/packing analysis carried out.

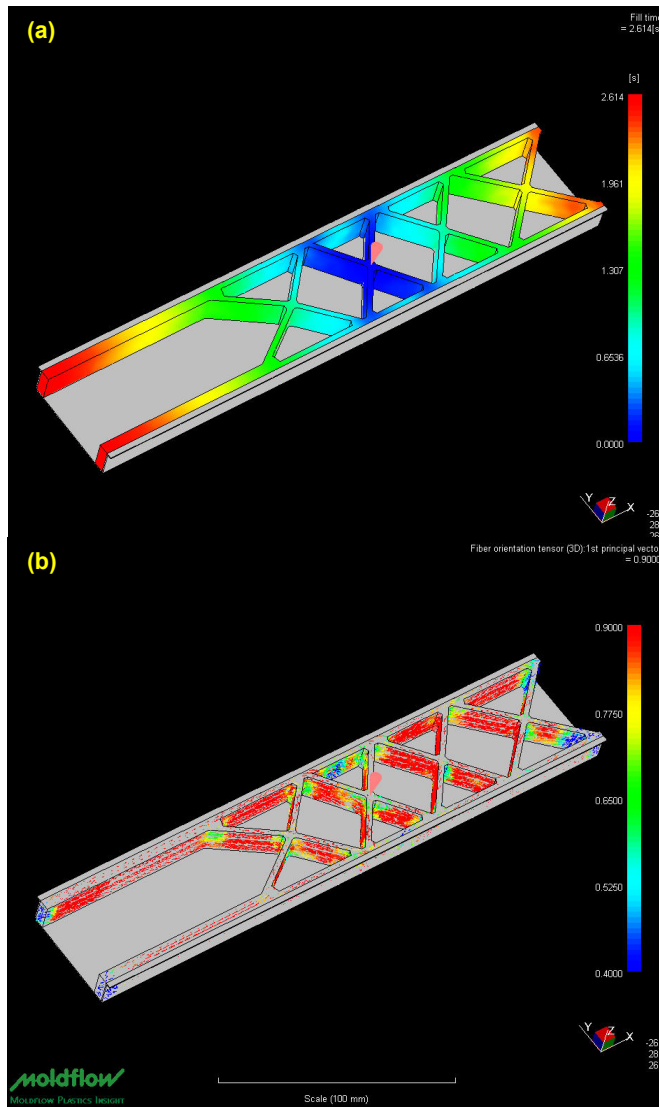


Fig.7 The results of an Injection over-molding manufacturability analysis for the prototypical PMH component: (a) mold filling time, (b) fiber orientation; (c) in-cavity first principal stress and (d) locations of weld lines and air traps.

An example of the results obtained in a typical Moldflow based mold-filling analysis is displayed in Figure 7(a)-(d). The analysis carried out in the present work was particularly useful for identification of the minimal manufacturable rib-wall thickness, the optimal locations of injection points (gates) with respect to minimization of the effects of unbalanced flow, failure-conductive weld-lines, air traps, etc. Overall, it was found that the use of the PMH technology can reduce the weight of the injection over-moldable prototypical PMH component by ~10-15% with respect to the all-metal

counterpart. In other words, the results obtained suggest that from the stand point of meeting the functional (load-bearing) requirements the prototypical PMH component analyzed in the present work could be 15-20% lighter than its all-metal counter part. However, the component manufacturability by injection over-molding entails that some sections of the PMH components are made thicker to prevent formation of the flaws in the component. It should be noted that the injection over-molding analysis carried out in the present work was done under the condition that a Netstal commercial injection molding machine Model 4200H-2150 (with the following specifications: (a) The injection unit - maximum machine injection stroke = 248mm, maximum machine injection rate = 5024 cm³/s, machine screw diameter = 80 mm; (b) The hydraulic unit - maximum machine hydraulic pressure = 17.5MPa, intensification ratio = 10.0, machine hydraulic response time = 0.2s; and (c) The clamping unit - maximum machine clamp force = 3800 ton.) is used and that the total cycle time is less than 5 seconds. Clearly, if an injection-molding machine with a higher capacity is used and the maximum acceptable cycle time is increased further weight savings can be gained.

It should be noted that in the structural optimization analysis carried out in the previous sections, it was assumed that the injection-molded thermoplastic material is isotropic. The results displayed in Figure 7(b) show that the reinforcing fibers are highly aligned causing the material to become anisotropic. It was hence necessary to validate the final design of the PMH component. With the anisotropy of the thermoplastic material taken into account, the final designs for all the loading and design-requirement cases, have been found to still satisfy the optimization constraints. Ideally, one would like to carry out additional (size and shape) optimization analyses under the assumption that the material anisotropy will not change. This was not done in the present case since, as pointed out earlier, size and shape optimizations typically yield only minor additional weight savings.

In our ongoing work [69], the concept of manufacturability has been extended to include the consideration of the PMH-component manufacturing cost. While a detailed discussion of the total manufacturing cost analysis is beyond the scope of the present paper, a brief account of the procedure used in our ongoing work [69] is presented in the remainder of this section.

The cost-based manufacturability analysis includes the consideration of overall benefit to the vehicle structural sub-system or total vehicle brought about by the use of the PMH component. In other words, for each design optimization scheme (e.g. lower weight, improved stiffness, etc.), the resulting financial benefits are being assessed and compared with the added manufacturing cost. Toward that end, systemic benefit functions are being developed to evaluate differences in manufacturing costs with respect to the economic benefits of design improvement. In the present paper, however, a design constraint that the PMH-component manufacturing cost should not exceed the manufacturing cost of the current all-metal component is imposed, for simplicity. Likewise, in the present paper, the injection over-molding process is constrained to release in a direction normal to the PMH-component longitudinal direction, precluding the need for independent side actions or lateral feature tooling. This prevents the cost of the independent slide from outweighing any manufacturing cost saving, and introduction of new levels of complexity to the design-optimization process. Additional mold actions are, however, being considered in our on-going work to explore the possibilities of alternate polymer sub-component architecture with more substantial weight savings [71].

The total manufacturing cost, C_m , is segregated into contributing components as follows:

$$C_m = C_{mat} + C_{tool} + C_{op} + C_{maint} \quad (2)$$

where C_{mat} , C_{tool} , C_{op} and C_{maint} are respectively the material, tooling, burdened operating (including labor and overhead) and maintenance costs (for the injection over-molding process in the present case).

The (marginal) material cost, C_{mat} , is defined as a difference in the cost of glass-fiber reinforced nylon (used in the injection over-molding ribbed sub-component) and the cost of steel (used in the removed upper stamped sub-component). The costs of nylon and steel are sub-component weight-specific and also depend on the respective (weight) specific material cost. The specific material costs are determined using the so called “*tiered-volume pricing model*”, i.e. they are based on total planned production volume for the PMH component.

Tooling manufacturing cost, C_{tool} , is assessed using the volume of material removed in mold manufacture, a material-specific cost factor based on material removal rate. A mold-complexity $C_{op} = (t_{inj} + t_{pack} + t_{solid} + t_{op-cl})c_L$ factor (accounts for the number of independent machining operations needed to produce features such as multiple gates and different runner geometries). The complexity factor was assessed using the mold design and manufacturing collaborative methods [72], and the mold-manufacture cost modeling approach [73].

The operating cost, C_{op} , is assessed using the manufacturability-analysis results presented in Section III.4 as:

$$C_{op} = (t_{inj} + t_{pack} + t_{solid} + t_{op-cl})c_L \quad (3)$$

where t_{inj} , t_{pack} , t_{solid} , and t_{op-cl} are respectively the injection, packing, solidification and open/eject/close times and c_L is the specific burdened labor rate. In other words, the operating cost consists of a fixed labor rate applied to the total cycle time. Design-specific and part-volume dependent components of the operating-cost function scale with the injection, packing and solidification times, and are determined by the MoldFlow injection-molding simulations discussed earlier. In other words, the component-quality and cost based manufacturability analyses are interfaced through the operating-cost function.

A maintenance cost function, C_{maint} , is developed which includes the effects of mold complexity, the volume of material per part, the frequency and the duration of mold polishing and lubrication operations, the cost of maintenance-consumed materials. While assessing the maintenance cost, the following main assumptions are made: (a) the injection over-molding equipment is available and functionally integrated to the manufacturing process; (b) the surface mechanical and chemical pre-treatment processes are fixed in cost; and (c) the cost of additional mold features such as multiple gates can be accounted for using the mold-complexity factor.

3.5 Automated Optimization and Manufacturability Analyses

In our ongoing work [] our effort is being made to develop computational capabilities which can be used, for a given type of loading (i.e. axial compression, bending, torsion) and a given functional (load-bearing) requirements (i.e. stiffness, strength, buckling

resistance) and manufacturability requirements, to automatically generate the optimal final design of the BIW load-bearing PMH component. A detailed account of these computational capabilities will be reported in our future communications. These capabilities are centered around the use of various script files and macros which enable batch-mode interaction with the CAD, the pre-processor, the analysis, the optimization and the process-modeling tools. The entire automated optimization and manufacturability analyses is orchestrated using Matlab, a general purpose mathematical and simulation package from MathWorks [70]. A schematic of the major steps used in this procedure is shown in Figure 8.

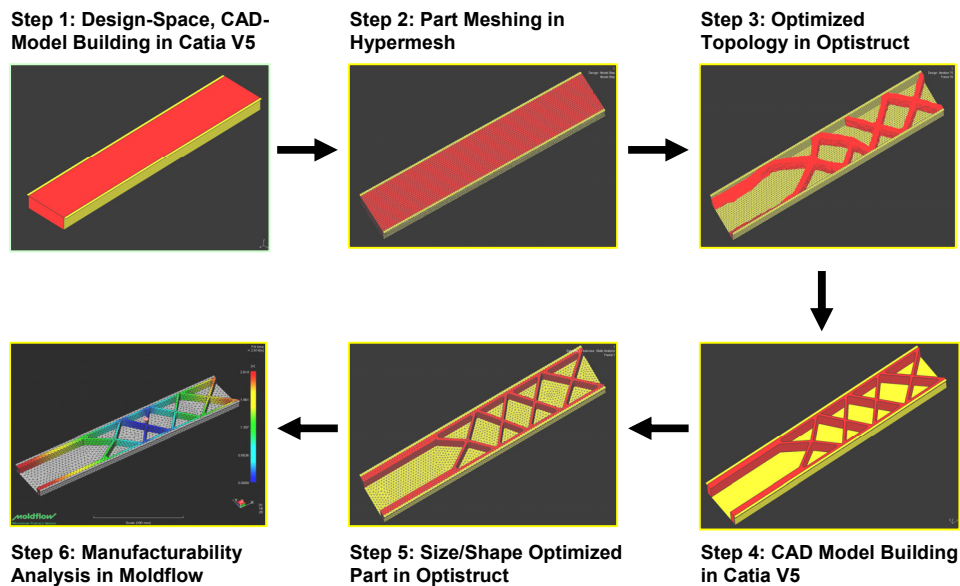


Fig.8 Key Steps used in the automated BIW load-bearing PMH-component optimization procedure.

3.6 System- integration based Design Optimization

Within the on-going work [69], a system-integration based design-optimization of the BIW load-bearing PMH components is being developed. Within this approach, ramifications of the design modifications are assessed not only with respect to the performance of the component in question but also relative to the performance of the associated sub-assembly and that of the total vehicle. The associated design-optimization procedure then involves the assessment of several total-vehicle performance functions such as those reflecting vehicle dynamics and stability, noise, vibration and harshness aspects, interactions with of the vehicle electronics, environmental impact, component-material segregation, recycling and recovery, etc.

The results of the system-integration based design optimization of the BIW load-bearing PMH-components will be presented in a future communication.

4. Summary and Conclusions

Based on the results obtained in the present work, the following summary and main conclusions can be made:

1. The present work illustrates how geometrical-modeling, topology, size and shape optimization and manufacturing-process modeling methods and tools may be used in the design of body-in-white (BIW) load bearing polymer/metal hybrid components.
2. The technology is being successfully used in an ongoing research project aimed at the development of short lead-time lightweight automotive BIW structural components with efficient stiffness, strength and buckling performance.
3. For a proto-typical BIW load-bearing PMH component analyzed in the present work, the extent of geometrical and material non-linearities was found to be relatively small so that buckling-resistance based design can be carried out using the linearized eigenvalue buckling analysis without a need for a computationally quite more intensive non-linear buckling analysis.
4. The concept of component manufacturability has been generalized to append cost-effective manufacturing to the notion of manufacturability of a defect-free high quality component.

Acknowledgement

The material presented in this paper is based on work conducted as a part of the project "Lightweight Engineering: Hybrid Structures: Application of Metal/Polymer Hybrid Materials in Load-bearing Automotive Structures" supported by BMW AG, München, Germany.

References:

- [1]. BMW Lightweight Technology: Achieving the Right Ecological Balance, BMW AG July 29, 2003.
- [2]. J. Zoellner and J. A. Evans, *Annual Technical Conference*, 1-4(2002).
- [3]. Plastic-Metal Hybrid Material, <http://www.hbmedia.net/polymotive/polymotive/2003/01/articles/frontend1.shtml>.
- [4]. D. Recktenwald, *Mach. Des.*, 21(2005)124-126.
- [5]. M. Grujicic, V. Sellappan, G. Arakere, N. Seyr and M. Erdmann, *J. Mater. Process. Technol.*, submitted for publication.
- [6]. Altair Engineering, Inc. www.altair.com.
- [7]. Abaqus, Inc. www.hks.com.
- [8]. MoldFlow Corporation, www.moldflow.com.
- [9]. P. Y. Papalambros and D. J. Wilde, *Principles of Optimal Design: Modeling and Computation*, 2000.
- [10]. L. Gil and A. Andreu, *Comput. Struct.*, 9(2001)681-689.
- [11]. N. L. Pedersen and A. K. Nielsen, *Struct. Multidiscip. Optim.*, 25(2003)436-445.
- [12]. H. Nishigaki, S. Nishiwaki, T. Amago, K. Yoshio and N. Kikuchi, *SAE Technical Paper*, No. 2001-01-0768, Pennsylvania.
- [13]. H. Fredricson, T. Johansen, A. Klarbring and J. Petersson, *Struct. Multidiscip. Optim.*, 25(2003)199-214.
- [14]. Takezawa, S. Nishiwaki, K. Izui and M. Yoshimura, *Proceedings of the ASME 2003 Design Engineering and Technical Conferences*, DETC2003/DAC-48773.

- [15]. Takezawa, S. Nishiwaki, K. Izui, M. Yoshimura, H. Nishigaki, and Y. TsuRumi, *Concurr. Eng. Res. Appl.*, 121(2005)29-42.
- [16]. Takezawa, S. Nishiwaki, K. Izui and M. Yoshimura, *Proceedings of the ASME 2004 Design Engineering and Technical Conferences*, DETC2004-57369.
- [17]. M. P. Bendsoe and N. Kikuchi, *Comput. Methods Appl. Mech. Eng.*, 71(1988)197-224.
- [18]. G. I. N. Rozavany, *Struct. Multidiscip. Optim.*, 21(2001)90-108.
- [19]. K. Suzuki and N. Kikuchi, *Comput. Methods Appl. Mech. Eng.*, 9(1991)291-318.
- [20]. R. Diaz and N. Kikuchi, *Int. J. Numer. Methods Eng.*, 3(1992)487-1502.
- [21]. Z.D. Ma, N. Kikuchi and H.C. Cheng, *Comput. Methods Appl. Mech. Eng.*, 121(1995)259-280.
- [22]. N. L. Pedersen, *Struct. Multidiscip. Optim.*, 20(2000)2-11.
- [23]. R. R. Mayer, N. Kikuchi and R. A. Scott, *Int. J. Numer. Methods Eng.*, 39(1996)1383-1403.
- [24]. R. R. Mayer, *Proceedings of the ASME 2001 International Mechanical Engineering Congress and Exposition*, IMECE2001/AMD-25458.
- [25]. J. Luo, H. C. Gea and R. J. Yang, *AIAA Paper*, AIAA-2000-4770.
- [26]. R. R. Mayer, D. Maurer and C. Bottcher, *Proceedings of the ASME 2000 Design Engineering and Technical Conferences*, DETC2000/DAC-14292.
- [27]. H. C. Gea and J. Luo, *Proceedings of the ASME 2001 Design Engineering and Technical Conferences*, DETC2001/DAC-21060.
- [28]. A. Soto, *Proceedings of the ASME 2001 Design Engineering and Technical Conferences*, DETC-2001/DAC-21126,
- [29]. A. Soto, *Proceedings of the ASME 2001 International Mechanical Engineering Congress and Exposition*, IMECE2001/AMD-25455.
- [30]. K.K. Bae, S. W. Wang and K. K. Choi, *Proceedings of The Second China-Japan-Korea Joint Symposium on Optimization of Structural and Mechanical Systems (CJK-OSM 2)*, 647-653.
- [31]. G. Kharmanda, N. Olhoff, A. Mohamed and M. Lemaire, *Struct. Multidiscip. Optim.*, 265(2004)295-307.
- [32]. M. Bremicker, M. Chirehdast, M. Kikuchi and P. Y. Papalambros, *Mech. Struct. Mach.*, 19(1991)551-587.
- [33]. S. Chen and D. Tortorelli, *Struct. Optim.*, 13(1997)81-94.
- [34]. R. T. Haftka and R.V. Grandhi, *Comput. Methods Appl. Mech. Eng.*, 57(1986)91-106.
- [35]. D. Belegundu and S. D. Rajan, *Comput. Methods Appl. Mech. Eng.*, 66(1988)87-106.
- [36]. *NASTRAN*
- [37]. H. Azegami, M. Shimoda, E. Katamine and Z. C. Wu, *Computer Aided Optimization Design of Structures IV, Structural Optimization*, (1995)51-58,
- [38]. R. Inzarulfaisham and H. Azegami, *Struct. Multidiscip. Optim.*, 27(2004)210-217.
- [39]. Y. Kawabe, S. Yoshida, S. Saegusa, I. Kajiwara and A. Nagamatsu, *J. Mech. Des.*, 121(1999), 188-194.
- [40]. K. Inoue, M. Yamanaka and M. Kihara, *J. Mech. Des.*, 124(2002)518-523.
- [41]. J. Sobieszcanski-Sobieski, S. Kodiyalam and R. Y. Yang, *Struct. Multidiscip. Optim.*, 22(2001) 295-306.
- [42]. R. J. Yang, C. H. Tho, C. C. Wu, D. Johnson and J. Cheng, *Proceedings of the ASME 1999 Design Engineering and Technical Conferences*, DETC99/DAC-8590.
- [43]. Q. Shi, I. Hagiwara and F. Takashima, *Proceedings of the ASME 1999 Design Engineering and Technical Conferences*, DETC99/DAC-8635.
- [44]. R. J. Yang, L. Gu, L. Liaw, C. Gearhart, C. H. Tho, X. Liu and B.P. Wang, *Proceedings of the ASME 2000 Design Engineering and Technical Conferences*, DETC2000/DAC-14245.
- [45]. R. J. Yang, N. Wang, C. H. Tho, J. P. Bobineau and B. P. Wang, *Proceedings of the ASME 2001 Design Engineering and Technical Conferences*, DETC2001/DAC-21012.
- [46]. M. Redhe and L. Nilsson, *AIAA Paper*, AIAA-200-2-5536.
- [47]. J. Han and K. Yamada, *AIAA Paper*, AIAA-2000 4750.
- [48]. H. Kurtaran, T. Omar and A. Eskandarian, *Proceedings of the ASME 2001 International Mechanical Engineering Congress and Exposition*, IMECE2001/AMD-25452.
- [49]. S. Chen, *Finite Elem. Anal. Design*, 37(2001)431-446.
- [50]. T. Mase, J. T. Wang, R. Mayer, K. Bonello and L. Pachon, *Proceedings of the ASME 1999 Design Engineering and Technical Conferences*, DETC99/DAC-8572.

- [51]. R. J. Yang, L. Gu, C. H. Tho and J. Sobieski, *Proceedings of the American Institute of Aeronautics and Astronautics 2001 Conference*, (2001)688-698, AIAA Paper No. AIAA-2001-1273.
- [52]. Grindeanu, K. K. Choi and K.H. Chang, *J. Mech. Des.*, 120(1998)491-500.
- [53]. J. Dong, K. K. Choi and N. H. Kim, *J. Mech. Des.*, 126(2004)527-533.
- [54]. J. S. Liu and L. Hollaway, *Struct. Multidiscip. Optim.*, 16(1998)29-36.
- [55]. Lund, H. Miller and L. A. Jakobsen, *Struct. Multidiscip. Optim.*, 25(2003)383-392.
- [56]. L. L. Howell, S. S. Rao and A. Midha, *J. Mech. Des.*, 116(1994)1115-1121.
- [57]. M. B. Parkinson, L. L. Howell and J. Cox, *Proceedings of the ASME 1997 Design Engineering Technical Conferences*, DETC97/DAC-3763.
- [58]. Xu and G. K. Anamthasuresh, *J. Mech. Des.*, 125(2003)253-261.
- [59]. D.A.K. Saitou, Wang and S. J. Wou, *J. Microelectromech. Syst.*, 9(2000)336-346.
- [60]. L. Saggere, S. Kota and S. B. Crary, *Proceedings of the ASME 1994 Winter Annual Meeting*, (1994)671-675.
- [61]. Y. H. Cho and A. P. Pisano, *Proceedings of the ASME 1990 Winter Annual Meeting*, (1990)31-49.
- [62]. W. Ye, S. Mukherjee and N. C. MacDonald, *J. Microelectromech. Syst.*, 7(1998)16-26.
- [63]. D. Jensen, S. Mutlu, S. Miller, K. Kurabayashi and J. J. Allen, *J. Microelectromech. Syst.*, 123(2003)373-383.
- [64]. J. Tu, K. K. Choi and Y. H. Park, *J. Mech. Des.*, 121(1999)557-564.
- [65]. Y. Murotsu, S. Shao, N. Kogiso and H. Tomioka, *American Society of Civil Engineers*, (1996)145-156.
- [66]. D. Youn and K. K. Choi, *J. Mech. Des.*, 125(2003)221-232.
- [67]. X. Chen, T. K. Hasselman and D. J. Neill, *Proceedings of the 38th AIAA/ASME/ASCE/AHS/ASC Structures, Structural Dynamics, and Materials Conference and Exhibit*, 1997, AIAA-97-1403.
- [68]. Dassault Systems, www.3ds.com.
- [69]. M. Grujicic, *Ongoing research*, Clemson University, 2007.
- [70]. MATLAB, *The Language of Technical Computing*, 7th Edition, 2006
- [71]. G. Banerjee and S. K. Gupta, *Geometric Modeling and Processing.*, (2006)500-513.
- [72]. R. C. Creese and T. Patrawala, *Proceedings of the SPIE - The International Society for Optical Engineering*, 3517(1998)172-182.
- [73]. P. Krajcnik and J. Kopac, *J. Mater. Process. Technol.*, 157-158(2004)543-552